Available online at www.sciencedirect.com
ScienceDirect
Virology 374 (2008) 444–452
VIROLOGY
www.elsevier.com/locate/yviro

VP1u phospholipase activity is critical for infectivity of full-length parvovirus B19 genomic clones

Claudia Filippone [a,1], Ning Zhi [a,*,1], Susan Wong [a], Jun Lu [a], Sachiko Kajigaya [a], Giorgio Gallinella [b], Laura Kakkola [c], Maria Söderlund-Venermo [c], Neal S. Young [a,2], Kevin E. Brown [d,2]

[a] *Hematology Branch, National Heart, Lung, and Blood Institute, National Institute of Health, USA*
[b] *Department of Clinical and Experimental Medicine, University of Bologna, Italy*
[c] *Department of Virology, Haartman Institute, University of Helsinki, Finland*
[d] *Centre for Infections, Health Protection Agency, London, UK*

Received 9 November 2007; returned to author for revision 14 December 2007; accepted 4 January 2008
Available online 5 February 2008

Abstract

Three full-length genomic clones (pB19-M20, pB19-FL and pB19-HG1) of parvovirus B19 were produced in different laboratories. pB19-M20 was shown to produce infectious virus. To determine the differences in infectivity, all three plasmids were tested by transfection and infection assays. All three clones were similar in viral DNA replication, RNA transcription, and viral capsid protein production. However, only pB19-M20 and pB19-HG1 produced infectious virus. Comparison of viral sequences showed no significant differences in ITR or NS regions. In the capsid region, there was a nucleotide sequence difference conferring an amino acid substitution (E176K) in the phospholipase A_2-like motif of the VP1-unique (VP1u) region. The recombinant VP1u with the E176K mutation had no catalytic activity as compared with the wild-type. When this mutation was introduced into pB19-M20, infectivity was significantly attenuated, confirming the critical role of this motif. Investigation of the original serum from which pB19-FL was cloned confirmed that the phospholipase mutation was present in the native B19 virus.

Keywords: Parvovirus B19; PLA_2-like motif; Infectious clone

Introduction

Parvovirus B19 (B19V), a member of the genus *Erythrovirus* of the family *Parvoviridae*, is a pathogenic virus distributed worldwide in the human population (Young and Brown, 2004). B19V is highly erythrotropic: infection of human erythroid progenitor cells leads to cytotoxicity and interruption of erythrocyte production (Mortimer et al., 1983). The physiological conditions of the host and the extent of the immune antiviral response then contribute to the evolution and clinical manifestation of the infection (Young and Brown, 2004). Infection causes fifth disease in children (Anderson et al., 1985, 1983), polyarthropathy syndrome in adults (Matsumura, 2001; Moore, 2000), transient aplastic crisis in patients with underlying chronic hemolytic anemia (Pattison et al., 1981; Serjeant et al., 1981), and chronic anemia due to persistent infection in immunocompromised patients (Kurtzman et al., 1989, 1988). Infection during pregnancy can lead to hydrops fetalis with possible fetal loss (Kinney et al., 1988) and/or congenital infection (Brown et al., 1993b).

In common with other parvoviruses, B19V has a small (22 nm), nonenveloped, icosahedral capsid, encapsidating a limited single-stranded DNA genome (5596 nucleotides (nt)). The ends of the genome are long inverted terminal repeats (ITRs) of 383 nt, of which the distal 365 nt forms an imperfect palindrome (Deiss et al., 1990). Transcription of the B19 viral genome is controlled by a single promoter (p6) located at map unit 6, which regulates the synthesis of all nine viral transcripts (Blundell et al., 1987; Ozawa et al., 1987). The single nonspliced

* Corresponding author. Bldg. 10/CRC, Rm. 3E5272 National Institutes of Health, 9000 Rockville Pike, Bethesda, MD 20892, USA. Fax: +1 301 496 8396.
E-mail address: zhin@nhlbi.nih.gov (N. Zhi).
[1] These authors contributed equally to this work.
[2] These authors equally supervised the project.

0042-6822/$ - see front matter © 2008 Elsevier Inc. All rights reserved.
doi:10.1016/j.virol.2008.01.002

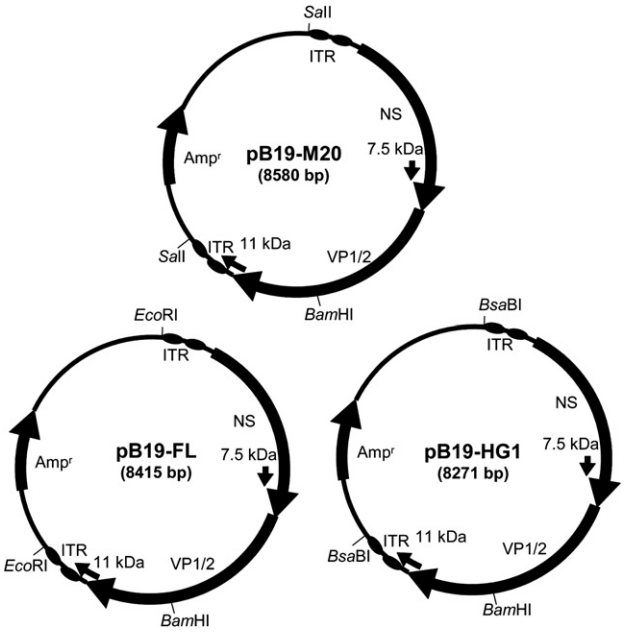

Fig. 1. Schematic representation of three full-length B19V genomic clones. The three full-length B19V genomic clones, pB19-M20, pB19-FL and pB19-HG1, were obtained from the B19V J35 isolate (GenBank Accession no. AY386330), the NAN isolate (GenBank Accession no. AY504945) and the HV isolate (GenBank Accession no. AF162273), respectively. The recombinant plasmids were constructed using different plasmid vectors: pB19-M20, pPRoEX HTb vector; pB19-FL, pLITMUS19 vector; and pB19-HG1, pUC18 vector. Arrows indicate the genes in either B19V genome or vector, and shaded circles indicate the ITR at both ends of B19V genome. Important restriction enzyme sites for cloning and analyzing are labeled.

transcript encodes a nonstructural protein (NS) and, by a combination of different splicing events, the other eight transcripts encode the two capsid proteins (VP1 and VP2) and two smaller proteins (7.5 kDa and 11 kDa) of yet unknown function (Cotmore et al., 1986; Ozawa et al., 1987; St Amand et al., 1991). In addition, a short open reading frame (ORF) putatively encoding protein X is present in the VP1 region of the B19V genome. The B19V NS protein is a multifunctional protein; in addition to transregulation of the p6 promoter (Doerig et al., 1990; Raab et al., 2002), NS contains motifs for nucleoside triphosphate (NTP) binding and hydrolysis (Momoeda et al., 1994) associated with helicase activity, suggesting a role of NS in B19V DNA replication. Accumulating evidence also suggest that the NTP-binding motif of NS is involved in the induction of apoptosis in erythroid lineage cells during B19V infection (Moffatt et al., 1998). The major capsid protein, VP2, which comprises 95% of the capsid, is a 58-kDa protein. Earlier studies showed that VP2 expressed in insect cells self-assembles into virus-like particles (Kajigaya et al., 1991) and VP2 binds directly to blood group P antigen, the cellular receptor of B19 virus (Brown et al., 1993a). The minor capsid protein, VP1, differs from VP2 only in an N-terminal "unique region" (VP1u) composed of an additional 227 amino acids. (Ozawa and Young, 1987). The VP1u region elicits a dominant immune response (Saikawa et al., 1993; Rosenfeld et al., 1992; Ros et al., 2006) and has phospholipase A_2 (PLA_2) activity, which is necessary for B19V infection (Lu et al., 2006; Zadori et al., 2001). The two small proteins, 7.5 kDa and 11 kDa, are encoded by the small, abundant mRNAs of B19V and are unique among the parvoviruses characterized to date (Luo and Astell, 1993; St Amand et al., 1991; St Amand and Astell, 1993). The 11-kDa protein contains several proline-rich motifs that are conserved to Src homology 3 (SH3) binding domain of eukaryotic proteins (Fan et al., 2001). What functions the 11-kDa or 7.5-kDa protein play in B19V replication and/or pathogenesis are unknown. We previously defined the specific roles of these viral proteins in B19V infectivity by mutagenesis analysis of the B19V infectious clone (Zhi et al., 2004, 2006): null mutation of the NS and VP1 proteins or deletion of the terminal hairpin sequence completely abolished the viral infectivity, and a null mutant of 11-kDa protein was significantly attenuated (Zhi et al., 2004, 2006).

Three independent full-length clones (pB19-M20, pB19-FL and pB19-HG1) have been produced in three different laboratories (Zhi et al., 2004, 2006). We have previously shown that pB19-M20 produces infectious virus. However the other two full-length clones (pB19-FL and pB19-HG1) have not been proven to be infectious. In the present study, the infectivity of these full-length clones was evaluated in parallel by transfection and infection assays. Mutagenesis analysis showed that a single amino acid substitution (E176K) in the VP1u region of pB19-FL resulted in loss of PLA_2 activity and attenuation of viral infectivity.

Results

Cloning and sequencing analyses of full-length parvovirus B19 genomes

Three independent full-length clones (pB19-M20, pB19-FL and pB19-HG1) were produced using different strategies (Fig. 1).

```
pB19-M20 MSKESGKWWE SDDEFAKAVY QQFVEFYEKV TGTDLELIQI LKDHYNISLD NPLENPSSLF DLVARIKNNL KNSPDLYSHH FQSHGQLSDH PHALSSSSSH AEPRGEDAVL 110
pB19-FL  ---------- ---K------ ---------- ---------- ---------- ---------- ---------- ---------- ---------- ---------- ------N---
pB19-HG1 ---------- ---K------ ---------- ---------- ---------- ---------- ---------- ---------- ---------- ---------- ------N---
                                                    Parvovirus PLA2-like motif
pB19-M20 SSEDLHKPGQ VSVQLPGTNY VGPGNELQAG PPQSAVDSAA RIHDFRYSQL AKLGINPYTH WTVADEELLK NIKNETGFQA QVVKDYFTLK GAAAPVAHFQ GSLPEVPAYN 220
pB19-FL  ---------- ---------- ---------- ---------- ---------- ---------- -----K---- ---------- ---------- ---------- ----------
pB19-HG1 ---------- ---------- ---------- ---------- ---------- ---------- -----E---- ---------- ---------- ---------- ----------
                    ● ●●●●                ●●                    ●
pB19-M20 ASEKYPS                                                                                                              227
pB19-FL  -------
pB19-HG1 -------
```

Fig. 2. Alignment of amino acid sequences of VP1u regions of three full-length B19V genomic clones. Aligned positions of identical amino acids with the VP1u region of pB19-M20 are shown with dashed lines. A boxed area indicates the PLA_2-like motif conserved among members of the *Parvoviridae*. Solid circles indicate conserved catalytic residues and Ca^{2+}-binding sites critical for enzymatic activity. The numbers on the right indicate the positions of amino acid residues in the VP1u region of parvovirus B19 from the N terminus to C terminus.

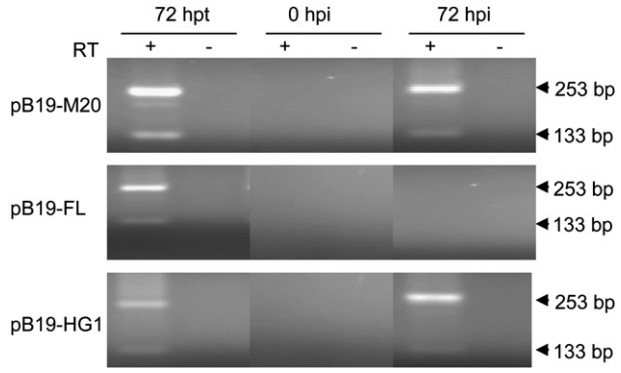

Fig. 3. Comparison of infectivity of three full-length B19V genomic clones by RT-PCR. Total RNAs were extracted from UT7/Epo-S1 cells at 72 h post-transfection (hpt), or 0 and 72 h post-infection (hpi). PCR was performed with a primer pair of B19-1 and B19-9. The products were analyzed by agarose gel electrophoresis. (+) or (−) indicates the presence or absence of the reverse transcriptase in the reaction, respectively. Numbers on the right indicate the respective amplicon sizes.

The entire B19V genomes in the three plasmids were sequenced. Since pB19-M20 had been shown to produce infectious virus, it was used for reference in the analyses of the DNA and protein sequences. Although the hairpin sequences were similar to each other among three B19V genomic clones, except for a deletion in pB19-HG1 at nucleotide 193, the secondary configurations of the hairpins in the palindromic regions were different: the hairpins in pB19-HG1 and pB19-FL had flip/flip and flop/flip structures, respectively, but the structures were flip/flop in pB19-M20.

Alignment of the primary amino acid sequences of the proteins showed eighteen substitutions among the B19V genomic clones (pB19-M20, pB19-FL and pB19-HG1) (Table 1). Fifteen of them were found in the VP2, NS and11-kDa proteins, and the putative X protein, but none were located in functionally important regions of the proteins (Ozawa et al., 1988; Fan et al., 2001). Among the three mutations found in VP1 (Fig. 2), a nucleotide point mutation (G3148A) of pB19-FL (corresponding to nt 3149 of pB19-M20) resulted in an amino acid substitution (E176K), which is proximate to the catalytic residues of the PLA_2-like motif in the VP1u region.

Production of infectious virus

We have previously shown that infectious virus was generated from the cells transfected with plasmid pB19-M20 (Zhi et al., 2004). In an attempt to determine if full-length clones pB19-FL and pB19-HG1 were also able to produce infectious virus, we used the supernatant prepared from the cell lysates of transfected cells to infect UT7/Epo-S1 cells, and detected spliced transcripts of viral capsid genes by RT-PCR as a marker for successful viral infection. The spliced transcripts were present in all samples (Fig. 3) at 72 h post-transfection. Immediately after inoculation of the clarified supernatant into the UT7/Epo-S1 cells, no RT-PCR product was detected in any of the samples (Fig. 3), indicating that there was no carry-over of the RNA from the transfected cells. At 72 h post-inoculation, spliced transcripts were detected in the samples derived from the cells transfected with pB19-M20 or pB19-HG1, but not with pB19-FL (Fig. 3); therefore both pB19-M20 and pB19-HG1 were infectious, but the production of infectious virus from the cells transfected with pB19-FL was below the level of detection.

Excision of B19V genome from the plasmids after transfection into permissive cells

During the replication of parvovirus B19, viral single-stranded DNA is converted to a double-stranded replicative form which

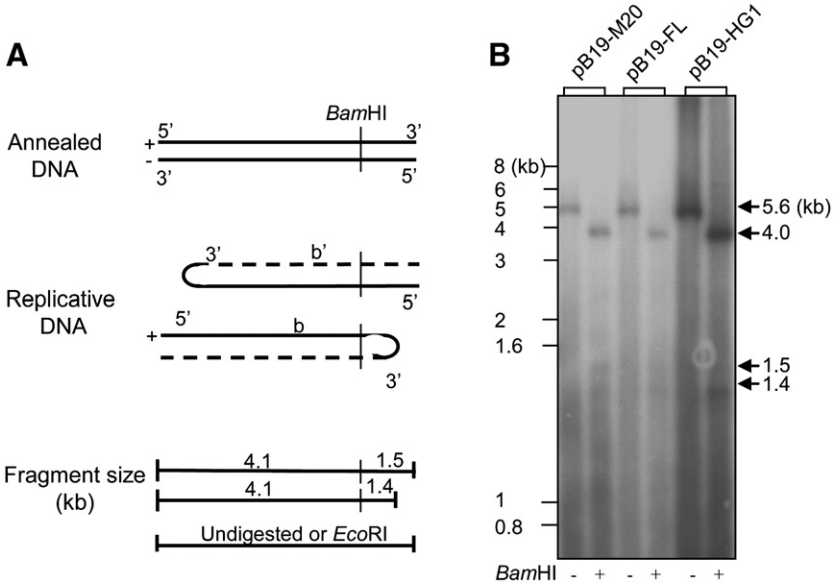

Fig. 4. Comparison of B19V replication following transfection of UT7/Epo-S1 cells with full-length B19V genomic clones. (A) Schematic representation of the replication of B19V genome. (B) Southern blot analysis of B19 genome replication. DNA was extracted by the Hirt method at 72 h post-transfection and analyzed by Southern blotting after digestion with EcoRI (−) or BamHI (+) in order to investigate the presence of characteristic replicative forms. The fragments were separated by agarose gel, transferred to a nylon membrane and hybridized with a ^{32}P-random-primed probe of the complete B19V genome.

has either an "extended" or a "turnaround" structure at the terminal region. These intermediate structures provide evidence for viral DNA replication and can be distinguished by BamHI restriction enzyme digestion (Fig. 4A). We performed Southern blot analysis to test whether the lack of production of infectious virus in pB19-FL was due to a defect in generation of progeny viral DNA.

The UT7/Epo-S1 cells were transfected with the DNA fragments containing full-length B19 genomes which were released from the plasmids by restriction enzyme digestions. After transfection, distinct doublets of 1.5 kb and 1.4 kb were detected in all the transfected cell samples digested with BamHI, (Fig. 4B). This result indicated that progeny viral DNA was generated from the cells transfected with the three full-length clones, including pB19-FL which was unable to produce infectious virus.

Viral capsid protein production

Viral capsid proteins in UT7/Epo-S1 cells transfected with each of three full-length clones (pB19-M20, pB19-FL or pB19-HG1) were compared using immunoblot analysis and immunofluorescence (IF) staining. For pB19-M20 and pB19-HG1, an expression level of the viral capsid protein was slightly lower than in the cells transfected with pB19-FL (Fig. 5A). When transfected UT7/Epo-S1cells were examined by IF staining with a monoclonal antibody specific for the viral capsid, the capsid proteins were detected in both nucleus and cytoplasm at 48 h post-transfection (Fig. 5B). No difference was found among the cells transfected with different plasmids.

VP1u PLA_2 activity is critical for the infectivity of full-length B19 clones

Comparison of amino acid sequences of capsid proteins among the three full-length B19V clones revealed a substitution

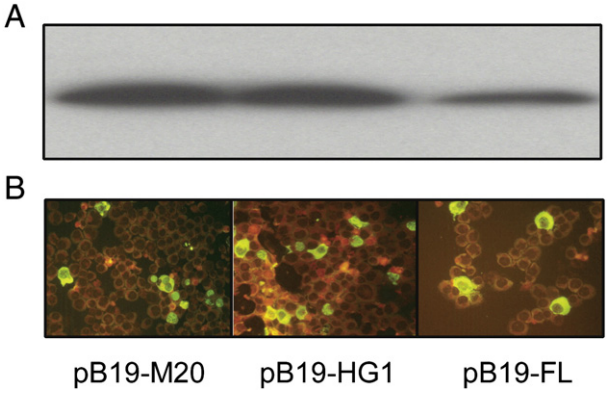

Fig. 5. Comparison of B19V capsid production following transfection of UT7/Epo-S1 cells with B19V full-length genomic clones. (A) Detection of the B19V VP2 capsid protein by immunoblotting. The samples were collected at 72 h post-transfection and tested by immunoblotting with MAB 8293 antibody to the viral capsid protein. Bands were visualized by chemiluminescence. (B) Detection of B19V capsid proteins by IF staining. UT7/Epo-S1 cells were transfected with pB19-M20, pB19-HG1 or pB19-FL, respectively. At 72 h post-transfection, the capsid proteins were detected using MAB 521-5D antibody and then FITC-labeled goat anti-mouse IgGs. Magnification ×750.

Table 1
Comparison of amino acid sequences among proteins encoded by three B19V full-length genomic clones

Protein names	Position of mutation [a]	Substitutions in three B19 full-length clones		
		pB19-m20 (J35 isolate)	PB19-FL (NAN isolate)	PB19-FL (HV isolate)
NS	57	L	F	F
	71	A	V	V
	11	F	L	L
	183	T	A	T
	205	F	F	I
	526	F	L	F
	558	P	P	S
VP1	14	E	K	K
	107	D	N	N
	176	E	K	E
	377	C	C	S
	574	T	T	P
VP2	150	C	C	S
	347	T	T	P
7.5 kDa		No change	No change	No change
11 kDa	7	D	D	G
	10	M	M	T
	54	I	V	V
X	51	A	V	A

[a] Positions and amino acid residues are described for each protein.

(E176K) in pB19-FL (Table 1), which resulted from a nucleotide point mutation (G3148A) of pB19-FL (corresponding to nt 3149 of pB19-M20) and is next to the catalytic residues of the PLA_2-like motif (Zadori et al., 2001) in the VP1u region. This mutation is unique to the pB19-FL clone and was not found in the B19V sequences which are available in the GenBank. Since the E176K substitution identified in pB19-FL clone was proximate to the catalytic residues of the PLA_2-like motif in the VP1u region, we tested the impact of the mutation on enzyme activity of PLA_2 by constructing a mutant based on the VP1u region of pB19-M20, in which the E176 was altered to K. In addition, to confirm the importance of conserved amino acid residues in the

Table 2
Impact of mutations in PLA_2 enzyme activity and B19V infectivity

Protein	Mutagenesis site [a]	PLA_2 activity [b]	Relative infectivity [c]
		μmol/min/ml	%
VPlu (pB19-M20)		0.187	100
P133R	C to G at nt 3021	0.001	20
H153A	C to G at nt 3080	0.005	62
	A to C at nt 3081		
A174G	C to G at nt 3144	0.001	2.1
D175A	A to C at nt 3147	0.001	1.2
E176K [d]	G to A at nt 3149	0.005	20
bv $sPLA_2$		0.63	0.63
TBS		0	

Result shown are the mean values for three independent experiments.

[a] Nucleotide numbers are based on the sequence of the J35 isolate (GenBank accession no. AY386330).

[b] Measured by the colorimetric kit. Protein concentration tested: recombinant proteins (VPlu, PI33R, HI53R, AI74G, DI75A and EI76K), 20 μg; bee venom (bv) secreted PLA_2, 10 ng.

[c] Relative infectivity $= \frac{\text{MT:fold change of viral transcript of day 0 vs day 3 post-infection}}{\text{WT:fold change of viral transcript of day 0 vs day 3 post-infection}} \times 100\%$

[d] Mutation EI76K converted the VPlu of pB19-M20 to pB19-FL.

Ca^{2+}-binding loop and enzyme catalytic site of B19V-PLA_2, four additional VP1u mutants, including P133R, H153A, A174G and D175A, were made and tested for their PLA_2 activities. All of the mutations in the Ca^{2+}-binding loop and enzymatic catalytic sites that were tested abolished PLA_2 activity (Table 2). In contrast to the wild-type (pB19-M20), PLA_2 activity was completely abolished when the E176K substitution identified in pB19-FL was introduced into the VP1u region of pB19-M20.

In order to test the impact of the PLA_2 activity on infectivity of B19V full-length clone, mutations P133R, H153A, A174G, D175A or E176K were introduced into the B19V infectious clone (pB19-M20). The five mutants were termed pB19-M20/PLA_2-P133R, pB19-M20/PLA_2-H153A, pB19-M20/PLA_2-A174G, pB19-M20/PLA_2-D175A and pB19-M20/PLA_2-E176K. After transfection of these mutants into UT7/Epo-S1 cells, the supernatants prepared from the cell lysates of transfected cells were used to infect $CD36^+$ erythroid progenitor cells ($CD36^+$ EPCs), and infectivity was quantitatively analyzed by real-time RT-PCR for the transcripts of the viral NS gene. In comparison with pB19-M20, the wild-type infectious clone, only 21% of relative infectivity was retained in the pB19-M20/PLA_2-E176K. Moreover, the relative infectivity of B19V mutants of pB19-M20/PLA_2-P133R, pB19-M20/PLA_2-H153A, pB19-M20/PLA_2-A174G and pB19-M20/PLA_2-D175A was decreased to 21, 62, 2.1, and 1.2%, respectively. Taken together, our data suggest that decreasing enzyme activity of PLA_2 due to the E176K mutation attenuated B19 viral infectivity. We also confirmed that VP1u-PLA_2 activity is critical to the infectivity of full-length B19V clones.

VP1u-PLA_2 mutation (E176K) identified in the native B19V NAN isolate

To exclude the possibility that the nucleotide point mutation (G3148A) of B19-FL clone was artifactually generated in the process of cloning, the VP1u region was PCR-amplified from a DNA sample of the patient serum (NAN) from which pB19-FL had been cloned. After TA cloning, inserts of 20 plasmids were sequenced: all contained the G3148A mutation, indicating that this mutation was carried in the original B19 virus. To compare the infectivity of the NAN isolate with the J35 isolate, the diluted patient sera containing similar numbers of B19V genome copies (10^8 copies/ml) were inoculated into UT7/Epo-S1 cells. Viral replication was evaluated by real-time PCR for viral capsid transcripts. At 72 h post-inoculation, the viral NS transcripts produced in the cells inoculated with the NAN isolate were approximately 100-fold less than those with the J35 isolate Fig. 6. In comparison with B19V J35 isolate, the relative infectivity of the NAN isolate was only 0.2%, indicating a marked attenuation of infectivity in the NAN isolate.

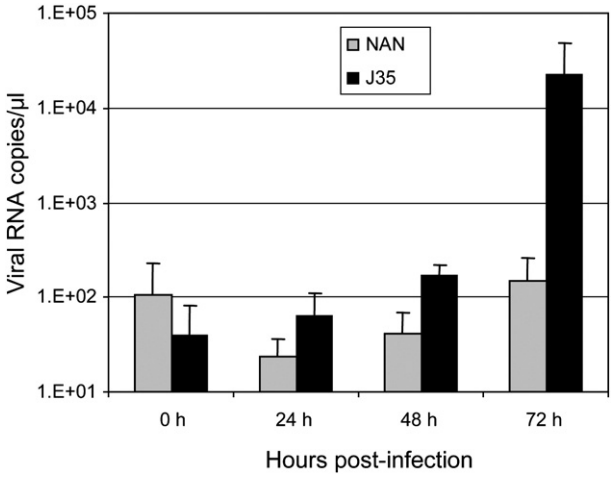

Fig. 6. Comparison of infectivity of the B19V J35 isolate and NAN isolates by real-time RT-PCR. The cells were inoculated with 50 genome copies/cell of virus. Total RNA was extracted from the cells at 0, 24, 48 and 72 h post-inoculation. The abundance of viral NS transcripts was measured by real-time RT-PCR. Quantitations are given as copy numbers of NS transcripts/µl of cDNA reaction. Results shown are mean values from three independent experiments.

Discussion

The availability of three full-length B19V genomic clones (pB19-M20, pB19-FL and pB19-HG1) permitted a systematic elucidation of molecular determinants of B19V pathogenicity. Clone pB19-M20 had been previously shown to be able to produce infectious virus after transfection into UT7/Epo-S1 cells (Zhi et al., 2004, 2006). Using a similar approach, we demonstrated that clone pB19-HG1 was infectious, but the infectivity of pB19-FL was much lower in comparison with those of pB19-M20 and pB19-HG1. Attenuated infectivity was also found in native virus (the NAN isolate) from which the pB19-FL was cloned. In order to determine why pB19-FL did not produce infectious virus, three viral sequences were compared: in the capsid region a nucleotide sequence difference, resulting in an amino acid substitution (E176K) in the PLA_2-like motif of the VP1u, was observed. The recombinant VP1u protein bearing this mutation had no catalytic activity compared with the wild-type recombinant proteins. Moreover, when this mutation was introduced into pB19-M20, there was a significant attenuation of infectivity, confirming a critical role of the PLA_2-like motif in viral infectivity.

Although a total of eighteen substitutions were found in viral proteins among pB19-M20, pB19-HG1 and pB19-FL, only three were unique in pB19-FL. In addition to the PLA_2 mutation (E176K) identified in VP1u, F526L in the NS protein and A51V in the X protein were present. Since no phenotypic change had been found between pB19-M20 and pB19-HG1, these three mutations unique for pB19-FL were likely responsible for the attenuation of infectivity in pB19-FL. NS is a multifunctional protein and plays important roles in regulation of the viral p6 promoter and DNA replication. The B19V NS sequence contains a conserved helicase motif (amino acids 306–344) and a putative NTP binding site (amino acids 326–393) (Momoeda et al., 1994). We have previously shown that a NS-null mutant was unable to replicate in permissive cells (Zhi et al., 2006). In this study, Southern blot analysis demonstrated that the replication form or newly synthesized viral DNA was detected in all cells transfected with the three B19V clones, suggesting that the substitution F526L in NS of pB19-FL had no impact on viral replication. No difference had been found between the

wild-type and the X protein null mutant in respect to infectivity and viral DNA replication (Zhi et al., 2006). Therefore, it is unlikely that the substitution A51V in the X protein had a significant impact on viral infectivity of pB19-FL.

We have reported that a VP1-null mutation completely abolished the infectivity of B19 virus (Zhi et al., 2006). The minor capsid protein, VP1, differs from VP2 only in the VP1u region composed of an additional 227 amino acids (Ozawa and Young, 1987). The main neutralizing epitopes of B19V are in VP1u region (Saikawa et al., 1993). Accessibility of the VP1u region in native viral capsids required a conformation change induced by acidification *in vitro* or cell-mediated stimulus during viral entry (Ros et al., 2006). Recently, a conserved PLA_2-like motif (HDXXY) was identified in the N-terminal extension of the VP1u region of members of the *Parvoviridae* (Zadori et al., 2001; Canaan et al., 2004), including B19V (Dorsch et al., 2002; Lu et al., 2006). Several amino acids in the highly conserved domain of the VP1u region share homologies to the Ca^{2+}-binding loop and catalytic site of secreted PLA_2. The residue P133 in the Ca^{2+}-binding loop, and H152, D153 and D175 in the catalytic site of B19V PLA_2 that corresponds to P21, H41, D42 and D63 in porcine parvovirus (PPV) are highly conserved in the PLA_2-like motif found in members of *Parvoviridae*. In PPV, mutation in these critical amino acid residues resulted in loss of PLA_2 activity and viral infectivity. In the present study, we constructed five PLA_2 mutants based on the B19V infectious clone (pB19-M20): the P133R mutant (the Ca^{2+}-binding loop), the H153A, A174G or D175A mutant (the enzyme catalytic site) or the E176K mutant (the VP1u region present in pB19-FL clone). The infectivity of viruses carrying these PLA_2 mutations was significantly attenuated, with relative infectivity ranging from 2 to 62%, implicating an important role of PLA_2 in the VP1 protein in the B19V life cycle. Although data obtained by *in vitro* PLA_2 activity assay showed that all mutations abolished the PLA_2 activity, the results of the infection assay revealed that the infectivity of viruses derived from these B19V mutant clones appeared to be variable. The viruses derived from two B19V infectious clones carrying point mutations in the enzyme catalytic site (A174G or D175A) completely lost infectivity. However, although PLA_2 enzyme activity was significantly decreased, viruses containing the point mutation P133R in the Ca^{2+}-binding loop and another mutation H153A in the enzyme catalytic site retained 21% and 62% of infectivity, respectively, in comparison with the wild-type infectious clone, pB19-M20. Similarly, viruses having the point mutation E176K were attenuated and retained only 21% of infectivity. Although E176 was less conserved, in comparison with other amino acid residues in the catalytic motif, conversion of an acidic residue (E) to a basic residue (K) likely disturbs the molecular structure of the enzyme. The attenuation of viral infectivity did not completely correlate with the reduction of PLA_2 enzyme activity of these mutants when tested by the *in vitro* assay. Although we cannot exclude the possibility that the VP1 unique region might have additional functions, the phenomena observed in our study likely implies a complexity of in vivo environment in which certain cellular factors may compensate for viral PLA_2 enzyme activity, and therefore help to retain the infectivity of these mutants to some degree. In order to test if the infectivity of the NAN isolate could be rescued by changing the VP1 unique region sequence to the wild-type sequence, we attempted to correct the E176K mutation in the VP1 unique sequence of pB19-FL (clone of NAN isolate) by insertion of the corrected sequence into the pB19-clone. However, due to the instability of the genome in the plasmid backbone, we were never been able to rescue a full-length corrected genome, and have therefore been unable to test the construct.

In immunocompetent individuals, B19V infection may be associated with arthralgia and arthropathy. The PLA_2-like motif in the exposed VP1u region may have a direct role in initiating and/or accelerating the inflammatory response in the synovial tissue and thus contributes to B19-associated arthropathy (Lu et al., 2006; Zadori et al., 2001). Studies of the original serum sample that was used as the source for cloning pB19-FL confirmed that the PLA_2 (E176K) mutant was present in the native virus (the NAN isolate). The B19V NAN isolate was identified in an individual without symptom of viral infection. The serum was found by real-time PCR to contain ~10^8 genome copies of B19/ml, much less than that of J35 (3.3×10^{13} genome copies/ml (Wong and Brown, 2006). The relative infectivity of the NAN isolate versus the J35 isolate was approximately 0.2%. The attenuation of the B19V NAN isolate for both viral replication and infectivity was at least partially due to the mutation in the PLA_2-like motif of its capsid protein. This naturally attenuated B19V could be an important candidate in development of an attenuated vaccine against B19V infection.

Materials and methods

Cells and viruses

UT7/Epo-S1 cells, a subclone of UT7/Epo (Shimomura et al., 1992) previously reported to have an increased sensitivity for parvovirus B19 were kindly provided by Kazuo Sugamura (Tohoku University Graduate School of Medicine, Japan). The cells were maintained in Iscove's modified Dulbecco's medium (IMDM, Mediatech, Herndon, VA) containing 10% fetal calf serum (FCS), 2 U/ml recombinant human (rhu) erythropoietin (Epo, Amgen, Thousand Oaks, CA) and antibiotics.

Human $CD36^+$ EPCs which are fully permissive for B19V infection were generated from G-CSF mobilized $CD34^+$ peripheral blood stems cells. The cells were cultured in a serum-free expansion medium containing a 1:5 dilution of BIT 9500 (Stem Cell Technologies, Vancouver, British Columbia, Canada) in alpha minimum essential medium (AMEM, Mediatech), obtaining a final concentration of 10 mg/ml of BSA, 10 μg/ml of rhu insulin, 200 μg/ml of iron-saturated human transferrin, 900 ng/ml of ferrous sulfate (Sigma, St. Louis, MO), 90 ng/ml of ferric nitrate (Sigma), 10 nM hydrocortisone (Sigma), 100 ng/ml of rhu SCF (Stem Cell Technologies), 5 ng/ml of rhu IL-3 (R&D Systems, Minneapolis, MN) and 3 U/ml of rhu EPO (Amgen).

The B19V J35 isolate (GenBank Accession no. AY386330) (Zhi et al., 2004), was obtained from the serum of a child with sickle cell anemia undergoing aplastic crisis and sent to the National Institutes of Health for diagnostic purposes. The serum was found to contain 3.3×10^{13} genome copies of B19/ml by

real-time PCR (Wong and Brown, 2006). The B19V NAN isolate (GenBank Accession no. AY504945), which was provided by Bernard Cohen (Health Protection Agency, London, UK), was obtained from a UK patient with asymptomatic B19V infection as part of a large scale screening of blood donors. The serum was found to contain ~10^8 genome copies of B19/ml by real-time PCR.

Cloning and sequencing of parvovirus B19 full-length genomic clones

Three full-length clones for parvovirus B19 were obtained from different sources. The plasmid pB19-M20 was constructed by separately cloning two halves of the virus resulting from a unique BamHI digestion; the halves were subsequently ligated to obtain the full-length B19V genome. pB19-M20 containing the full-length B19V genome of the J35 isolate has been proven to be infectious in our previous study (Zhi et al., 2004).

For pB19-HG1, the ITR and coding region of B19V genome were first PCR-amplified and separately cloned. After BssHII digestion, the fragments were joined together to form the full-length B19V genome. pB19-HG1 contained full-length B19V genome of the HV isolate (GenBank Accession no. AF162273).

For pB19-FL, B19V genome was digested with BssHII, ligated to the pLITMUS29 vector (New England Biolabs, MA) and transformed into competent DH5α cells (Brunstein et al., 2000). A positive clone, containing nt 185–5413 of B19V, was cut in half with BamHI. The missing 184 nt ends of the hairpins were synthesized as two pairs of 70–114 nt long oligos (with 11-nt overlaps in the middle and with BssHII and EcoRI sites at the inner and outer ends, respectively) for each end of the genome, which were annealed to each other and ligated to each half of the B19 clone. The final full-length B19V clone was obtained by joining the two genome halves by ligation of the excised left half into the plasmid containing the right half. pB19-FL contained full-length B19V genome of the NAN isolate.

Three different full-length B19V genomes cloned in the plasmids were sequenced using the BigDye terminator cycle sequencing kit (ABI-Perkin Elmer, Foster City, CA). The full-length sequences of both strands were obtained by primer walking. All DNA sequences and amino acid sequences of ORFs were analyzed using the Lasergene software (DNAStar, Inc., Madison, WI). DNA pairwise homology was determined by the Lipman–Pearson method with a Ktuple of 2, gap penalty of 4, and deletion penalty of 12. Multiple sequence alignments were performed by the Megalign program, using the Clustal method with a gap penalty of 10 and gap length penalty of 10.

Infection and transfection

For infection studies, 2×10^4 of UT7/Epo-S1 cells in 10 μl of IMDM were mixed with an equal volume of diluted viremic serum (J35 or NAN serum was diluted to contain 10^8 B19V genome copies/ml) and incubated at 4 °C for 2 h to allow for maximum virus–cell interaction. The cells were then diluted to 2×10^5 cells/ml in the culture medium, and incubated at 37 °C in 5% CO_2. Cells were harvested on day 3 post-infection and tested for evidence of infection by detection of viral transcripts and protein production.

Transfection of the UT7/Epo-S1 cells was performed as previously described (Zhi et al., 2004). The full-length B19 genome was released from the plasmids by restriction enzyme digestions with SalI (pB19-M20), EcoRI (pB19-FL) or BsaBI (pB19-HG1). The DNA fragments were separated by agarose gel electrophoresis, and the 5.6-kb B19V genome was excised and purified by using the QIAEX II Gel Extract kit (QIAGEN, Santa Clarita, CA). The cells (2×10^6) were transfected with 5 μg of purified B19 DNA using the AMAXA Cell Line Nucleofector™ kit (Amaxa, Gaithersburg, MD). The cells were harvested at various times post-transfection, and used for infection, DNA, RNA and immunofluorescence (IF) studies. For infection study, cells were harvested at 72 h post-transfection, washed free of inoculums using fresh culture medium, and cell lysate was prepared by three cycles of freeze/thaw. After centrifugation at 10,000 ×g for 10 min, a clarified supernatant was treated with RNase at a final concentration of 1 U/μl (Roche, Roswell, GA). UT7/Epo-S1 cells or $CD36^+$ EPCs (2×10^4) in 10 μl of culture medium were mixed with an equal volume of the clarified supernatant and incubated at 4 °C for 2 h to allow for maximum virus–cell interaction. The cells were then diluted to 2×10^5 cells/ml in the culture medium, and incubated at 37 °C in 5% CO_2. Cells were harvested on day 3 post-infection and tested for evidence of infection by detection of viral transcripts and protein expression.

RT-PCR and real-time RT-PCR

Total RNA was extracted from UT7/Epo-S1 cells (2×10^5) using RNA STAT60 (Tel-Test Inc., Friendswood, TX). Residual DNA was removed by DNase I (Promega, Madison WI) treatment at a final concentration of 90 U/ml for 15 min at room temperature. RNA was converted to cDNA using random hexamers and SuperScript II (Invitrogen, Carlsbad, CA), and RT-PCR for the spliced capsid transcripts was performed with primers B19-1 and B19-9 as previously described (Nguyen et al., 2002).

RNA transcripts were quantitated by real-time RT-PCR designed to amplify products in the NS regions using the QuantiTect Probe RT-PCR kit (Qiagen, Valencia, CA) as previously described (Wong and Brown, 2006). QuantiTect Probe RT-PCR master mix and QuantiTect RT mix were combined with 0.4 μM of the NS amplification primers (5′-GTTTTATGGGCCGCCA-AGTA-3′ and 5′-ATCCCAGACCACCAAGCTTTT-3′) and 0.2 μM NS probe (5′-FAM-CCATTGCTAAAAGTGTTCCA-BHQ1-3′). After an initial activation step of 15 min at 95 °C, 45 cycles of 15 s at 94 °C and 60 s at 60 °C were performed. The number of transcripts was estimated by comparison of the cDNA copy numbers with a standard curve of serial dilutions of pYT103 (Shimomura et al., 1992). To confirm extraction of RNA, and to normalize the numbers of transcripts per cell, real-time RT-PCR was performed using the same amplification condition, but with β-actin primers (5′-CACCCAGCACAATGAAG-3′ and 5′-GATCCACACGGAGTACT-3′) and β-actin probe (5′-JOE-

TCAAGATCATTGCTCCTCCTGAGCGC-BHQ-3′). A β-actin standard curve was obtained from serial dilutions of a plasmid containing an extended region of the β-actin-coding sequence.

Southern blot analysis of B19V DNA

DNA was extracted from transfected UT7/Epo-S1 cells (5×10^5) as previously described (Shimomura et al., 1992). Briefly, 5×10^5 cells were incubated with 100 mM NaCl, 10 mM Tris–HCl, pH 7.5, 0.5% sodium dodecylsulfate, 5 mM EDTA, and 200 μg/ml proteinase K overnight at 37 °C, followed by phenol–chloroform extraction. For some experiments high and low-molecular weight DNAs were separated by the Hirt method (Hirt, 1967). Purified DNA (400 ng) was digested with 20 U of BamHI (a single cut in B19) or EcoRI (no cut in B19) at 37 °C for 4 h, the fragments were then separated by agarose gel electrophoresis, transferred to a nylon membrane (Nylon+, Amersham, Piscataway, NJ), and hybridized with a ^{32}P-random-primed probe of the complete B19V coding region as previously described (Shimomura et al., 1992).

Immunoblot analysis and immunofluorescence staining of B19V capsid proteins

The procedure for immunoblotting was essentially the same as described elsewhere (Zhi et al., 1997). Briefly, cells were harvested at 72 h post-transfection and proteins were separated by 10% SDS-PAGE. The separated proteins were transferred to a nitrocellulose membrane (Invitrogen) and then blocked with Tris-buffered saline (TBS) buffer (150 mM NaCl, 50 mM Tris–HCl, pH 7.4) containing 5% milk and 0.05% Tween 20 at room temperature for 2 h to saturate protein-binding sites. Antigens were detected by incubation of the membrane with mouse monoclonal antibody MAB 8293 (Millipore Corporation, Billerica, MA) (1:1000 dilutions) to B19V capsid proteins, followed by incubation with peroxidase-conjugated anti-mouse antibody (1:100,000 dilutions; BD Biosciences Clontech, Palo Alto, CA). Bands were visualized by incubating the membrane with the SuperSignal chemiluminescent reagent (Pierce, Rockford, IL), and then exposing it to an X-ray film. The densities of detected bands were analyzed with a PhosphorImager (Molecular Dynamics, Sunnyvale, CA).

For IF staining, transfected cells were harvested and cytocentrifuged at 750×g for 8 min in a cytospin funnel (Shandon, Pittsburgh PA). The cells were fixed in acetone:methanol (1:1) at −20 °C for 5 min, washed twice in phosphate buffered saline (PBS), and incubated with mouse monoclonal antibody MAB 521-5D (Millipore Corporation) to conformational epitope of B19V capsid protein in PBS with 10% FCS for 1 h at 37 °C. For IF staining, a fluorescein isothiocyanate (FITC)-labeled goat anti-mouse IgG (BD Biosciences Clontech) was used as secondary antibody.

Cloning, site mutagenesis, expression, and purification of VP1u-region protein

The full-length VP1u region was cloned into a pET expression vector (Invitrogen) with V5 and 6× His epitopes at the carboxyl terminus. To obtain mutations in the PLA_2 motif of VP1u, site-directed mutagenesis was performed with the QuikChange Site-Directed Mutagenesis kit in accordance with the manufacturer's instructions (Stratagene, La Jolla, CA). All proteins were expressed in *Escherichia coli* BL21 Star strain (Invitrogen), after induction with 1 mmol/l isopropyl-β-D-1-thiogalactopyranoside for 5 h, and purified using the His Bind Purification kit (Novagen, San Diego, CA). The soluble purified proteins were dialyzed against TBS and concentrated using the Centriplus concentrator (10-kDa exclusion limit; Millipore) to give a final concentration of ~2 mg/ml.

PLA_2 catalytic activity

Recombinant B19V proteins were assayed for PLA_2 activity by the use of the PLA_2 Activity kit in accordance with the manufacturer's instructions (Cayman Chemical, Ann Arbor, Michigan), with dynamic colorimetric measurements (the optical density at 405 nm) determined every minute for 10 min. Results are expressed as micromoles per minute per milliliter.

Generation of B19V mutant genomes based on the infectious clones

The mutations of VP1u region were produced by site-directed mutagenesis of pB19-M20. Due to the instability of the ITRs, it was not possible to perform direct mutagenesis on plasmids containing the intact ITR sequences. Therefore, the B19V DNA fragments of interest were first subcloned into a plasmid vector and, after successful mutagenesis, were then reinserted into pB19-M20 as described in our previous study (Zhi et al., 2006). All final constructs were sequenced to confirm no unexpected mutation arisen from the processes of mutagenesis and cloning.

References

Anderson, M.J., Higgins, P.G., Davis, L.R., Willman, J.S., Jones, S.E., Kidd, I.M., Pattison, J.R., Tyrrell, D.A., 1985. Experimental parvoviral infection in humans. J. Infect. Dis. 152, 257–265.

Anderson, M.J., Jones, S.E., Fisher-Hoch, S.P., Lewis, E., Hall, S.M., Bartlett, C.L.R., Cohen, B.J., Mortimer, P.P., Pereira, M.S., 1983. Human parvovirus, the cause of erythema infectiosum (fifth disease)? [letter] Lancet i, 1378.

Blundell, M.C., Beard, C., Astell, C.R., 1987. In vitro identification of a B19 parvovirus promoter. Virology 157, 534–538.

Brown, K.E., Anderson, S.M., Young, N.S., 1993a. Erythrocyte P antigen: cellular receptor for B19 parvovirus. Science 262, 114–117.

Brown, K.E., Green, S.W., Antunez de Mayolo, J., Bellanti, J.A., Smith, S.D., Smith, T.J., Young, N.S., 1993b. Congenital infection with B19 parvovirus associated with constitutional anemia and pure red cell aplasia. Blood 82 (Suppl 1), 311a Ref type: abstract.

Brunstein, J., Soderlund-Venermo, M., Hedman, K., 2000. Identification of a novel RNA splicing pattern as a basis of restricted cell tropism of erythrovirus B19. Virology 274, 284–291.

Canaan, S., Zadori, Z., Ghomashchi, F., Bollinger, J., Sadilek, M., Moreau, M.E., Tijssen, P., Gelb, M.H., 2004. Interfacial enzymology of parvovirus phospholipases A2. J. Biol. Chem. 279, 14502–14508.

Cotmore, S.F., McKie, V.C., Anderson, L.J., Astell, C.R., Tattersall, P., 1986. Identification of the major structural and nonstructural proteins encoded by human parvovirus B19 and mapping of their genes by procaryotic expression of isolated genomic fragments. J. Virol. 60, 548–557.

Deiss, V., Tratschin, J.D., Weitz, M., Siegl, G., 1990. Cloning of the human parvovirus B19 genome and structural analysis of its palindromic termini. Virology 175, 247–254.

Doerig, C., Hirt, B., Antonietti, J.P., Beard, P., 1990. Nonstructural protein of parvoviruses B19 and minute virus of mice controls transcription. J. Virol. 64, 387–396.

Dorsch, S., Liebisch, G., Kaufmann, B., von Landenberg, P., Hoffmann, J.H., Drobnik, W., Modrow, S., 2002. The VP1 unique region of parvovirus B19 and its constituent phospholipase A2-like activity. J. Virol. 76, 2014–2018.

Fan, M.M., Tamburic, L., Shippam-Brett, C., Zagrodney, D.B., Astell, C.R., 2001. The small 11-kDa protein from B19 parvovirus binds growth factor receptor-binding protein 2 in vitro in a Src homology 3 domain/ligand-dependent manner. Virology 291, 285–291.

Hirt, B., 1967. Selective extraction of polyoma DNA from infected mouse cells. J. Mol. Biol. 26, 365–369.

Kajigaya, S., Fujii, H., Field, A., Anderson, S., Rosenfeld, S., Anderson, L.J., Shimada, T., Young, N.S., 1991. Self-assembled B19 parvovirus capsids, produced in a baculovirus system, are antigenically and immunogenically similar to native virions. Proc. Natl. Acad. Sci. U. S. A. 88, 4646–4650.

Kinney, J.S., Anderson, L.J., Farrar, J., Strikas, R.A., Kumar, M.L., Kliegman, R.M., Sever, J.L., Hurwitz, E.S., Sikes, R.K., 1988. Risk of adverse outcomes of pregnancy after human parvovirus B19 infection. J. Infect. Dis. 157, 663–667.

Kurtzman, G., Frickhofen, N., Kimball, J., Jenkins, D.W., Nienhuis, A.W., Young, N.S., 1989. Pure red-cell aplasia of 10 years' duration due to persistent parvovirus B19 infection and its cure with immunoglobulin therapy. N. Engl. J. Med. 321, 519–523.

Kurtzman, G.J., Cohen, B., Meyers, P., Amunullah, A., Young, N.S., 1988. Persistent B19 parvovirus infection as a cause of severe chronic anaemia in children with acute lymphocytic leukaemia. Lancet ii, 1159–1162.

Lu, J., Zhi, N., Wong, S., Brown, K.E., 2006. Activation of synoviocytes by the secreted phospholipase A2 motif in the VP1-unique region of parvovirus B19 minor capsid protein. J. Infect. Dis. 193, 582–590.

Luo, W., Astell, C.R., 1993. A novel protein encoded by small RNAs of parvovirus B19. Virology 195, 448–455.

Matsumura, M., 2001. Parvovirus-associated arthritis. Am. J. Med. 111, 241.

Moffatt, S., Yaegashi, N., Tada, K., Tanaka, N., Sugamura, K., 1998. Human parvovirus B19 nonstructural (NS1) protein induces apoptosis in erythroid lineage cells. J. Virol. 72, 3018–3028.

Momoeda, M., Wong, S., Kawase, M., Young, N.S., Kajigaya, S., 1994. A putative nucleoside triphosphate-binding domain in the nonstructural protein of B19 parvovirus is required for cytotoxicity. J. Virol. 68, 8443–8446.

Moore, T.L., 2000. Parvovirus-associated arthritis [In Process Citation] Curr. Opin. Rheumatol. 12, 289–294.

Mortimer, P.P., Humphries, R.K., Moore, J.G., Purcell, R.H., Young, N.S., 1983. A human parvovirus-like virus inhibits haematopoietic colony formation in vitro. Nature 302, 426–429.

Nguyen, Q.T., Wong, S., Heegaard, E.D., Brown, K.E., 2002. Identification and characterization of a second novel human erythrovirus variant, A6. Virology 301, 374–380.

Ozawa, K., Ayub, J., Hao, Y.S., Kurtzman, G., Shimada, T., Young, N., 1987. Novel transcription map for the B19 (human) pathogenic parvovirus. J. Virol. 61, 2395–2406.

Ozawa, K., Ayub, J., Kajigaya, S., Shimada, T., Young, N., 1988. The gene encoding the nonstructural protein of B19 (human) parvovirus may be lethal in transfected cells. J. Virol. 62, 2884–2889.

Ozawa, K., Young, N., 1987. Characterization of capsid and noncapsid proteins of B19 parvovirus propagated in human erythroid bone marrow cell cultures. J. Virol. 61, 2627–2630.

Pattison, J.R., Jones, S.E., Hodgson, J., Davis, L.R., White, J.M., Stroud, C.E., Murtaza, L., 1981. Parvovirus infections and hypoplastic crisis in sickle-cell anaemia. Lancet i, 664–665.

Raab, U., Beckenlehner, K., Lowin, T., Niller, H.H., Doyle, S., Modrow, S., 2002. NS1 protein of parvovirus B19 interacts directly with DNA sequences of the p6 promoter and with the cellular transcription factors Sp1/Sp3. Virology 293, 86–93.

Ros, C., Gerber, M., Kempf, C., 2006. Conformational changes in the VP1-unique region of native human parvovirus B19 lead to exposure of internal sequences that play a role in virus neutralization and infectivity. J. Virol. 80, 12017–12024.

Rosenfeld, S.J., Yoshimoto, K., Kajigaya, S., Anderson, S., Young, N.S., Field, A., Warrener, P., Bansal, G., Collett, M.S., 1992. Unique region of the minor capsid protein of human parvovirus B19 is exposed on the virion surface. J. Clin. Invest. 89, 2023–2029.

Saikawa, T., Anderson, S., Momoeda, M., Kajigaya, S., Young, N.S., 1993. Neutralizing linear epitopes of B19 parvovirus cluster in the VP1 unique and VP1–VP2 junction regions. J. Virol. 67, 3004–3009.

Serjeant, G.R., Topley, J.M., Mason, K., Serjeant, B.E., Pattison, J.R., Jones, S.E., Mohamed, R., 1981. Outbreak of aplastic crisis in sickle cell anaemia associated with parvovirus-like agent. Lancet ii, 595–597.

Shimomura, S., Komatsu, N., Frickhofen, N., Anderson, S., Kajigaya, S., Young, N.S., 1992. First continuous propagation of B19 parvovirus in a cell line. Blood 79, 18–24.

St Amand, J., Astell, C.R., 1993. Identification and characterization of a family of 11-kDa proteins encoded by the human parvovirus B19. Virology 192, 121–131.

St Amand, J., Beard, C., Humphries, K., Astell, C.R., 1991. Analysis of splice junctions and in vitro and in vivo translation potential of the small, abundant B19 parvovirus RNAs. Virology 183, 133–142.

Wong, S., Brown, K.E., 2006. Development of an improved method of detection of infectious parvovirus B19. J. Clin. Virol. 35, 407–413.

Young, N.S., Brown, K.E., 2004. Parvovirus B19. N. Engl. J. Med. 350, 586–597.

Zadori, Z., Szelei, J., Lacoste, M.C., Li, Y., Gariepy, S., Raymond, P., Allaire, M., Nabi, I.R., Tijssen, P., 2001. A viral phospholipase A2 is required for parvovirus infectivity. Dev. Cell 1, 291–302.

Zhi, N., Mills, I.P., Lu, J., Wong, S., Filippone, C., Brown, K.E., 2006. Molecular and functional analyses of a human parvovirus B19 infectious clone demonstrates essential roles for NS1, VP1, and the 11-kilodalton protein in virus replication and infectivity. J. Virol. 80, 5941–5950.

Zhi, N., Rikihisa, Y., Kim, H.Y., Wormser, G.P., Horowitz, H.W., 1997. Comparison of major antigenic proteins of six strains of the human granulocytic ehrlichiosis agent by Western immunoblot analysis. J. Clin. Microbiol. 35, 2606–2611.

Zhi, N., Zadori, Z., Brown, K.E., Tijssen, P., 2004. Construction and sequencing of an infectious clone of the human parvovirus B19. Virology 318, 142–152.